Hydrological Sciences Journal

ISSN: (Print) (Online) Journal homepage: https://www.tandfonline.com/loi/thsj20

Assessing climate change impact on French groundwater resources using a spatially distributed hydrogeological model

Jean-Pierre Vergnes, Yvan Caballero & Sandra Lanini

To cite this article: Jean-Pierre Vergnes, Yvan Caballero & Sandra Lanini (2023) Assessing climate change impact on French groundwater resources using a spatially distributed hydrogeological model, Hydrological Sciences Journal, 68:2, 209-227, DOI: 10.1080/02626667.2022.2150553

To link to this article: https://doi.org/10.1080/02626667.2022.2150553

Published online: 03 Jan 2023.

HYDROLOGICAL SCIENCES JOURNAL
2023, VOL. 68, NO. 2, 209–227
https://doi.org/10.1080/02626667.2022.2150553

Assessing climate change impact on French groundwater resources using a spatially distributed hydrogeological model

Jean-Pierre Vergnes [a], Yvan Caballero [b] and Sandra Lanini [b]

[a]Water, Environment, Processes and Analyses Division, BRGM – French Geological Survey, Orléans, France; [b]Water, Environment, Processes and Analyses Division, BRGM – French Geological Survey, Univ Montpellier, Montpellier, France

ABSTRACT

Today, large-scale modelling tools are needed for anticipating the expected impacts of climate change on hydrosystems and for planning mitigation measures. We developed a spatially-distributed model for the MARTHE (Modélisation d'Aquifères avec un maillage Rectangulaire, Transport et HydrodynamiquE; Modelling Aquifers with Rectangular cells, Transport and Hydrodynamics) hydrogeological modelling computer code as a preliminary tool for France, and carried out a first evaluation over a 10-year period, comparing observed and modelled time series of groundwater levels and river flows. Then, prospective hydrological simulations were undertaken using five regionalized climate simulations. The evaluation results show varying performance depending upon the regions and variables considered, but they provide encouraging perspectives. Future hydrological projections anticipate increased recharge by +15% on average over France, accompanied by increases in wetter/drier groundwater extreme events in the north/south by the 2070–2099 period compared to the 1976–2005 reference period. Based on these results, the MARTHE model can be considered a promising template for the construction of a nation-wide hydrological model.

ARTICLE HISTORY
Received 12 April 2022
Accepted 7 October 2022

EDITORS
A. Castellarin
S. Archfield
A. Fiori

ASSOCIATE EDITOR
M. Bianchi

KEYWORDS
modelling; climate; groundwater; France

1 Introduction

Groundwater is a key resource for domestic water supply, industry, and agriculture (Wada *et al.* 2010, Cuthbert *et al.* 2019). Therefore, assessing its evolution against future climate change is essential for planning appropriate mitigation measures. Traditionally, stakeholders have relied on numerical hydrological models at catchment scale for assessing the effect of future climate change over their area of interest (Crosbie *et al.* 2013, Amanambu *et al.* 2020, Muelchi *et al.* 2021). However, climate change mitigation strategies should be planned at the scale of regions or countries, which means there is a need to provide reliable information at these much larger scales in order to support the decision making process with scientifically based information.

In France, a decade ago, the Explore 2070 project was set up to provide an overview of climate change impact on water resources (Stollsteiner 2012, Chauveau *et al.* 2013). Impact on groundwater was assessed with independent regional hydrogeological models, which showed a decrease of recharge associated with longer droughts, lower water table levels, and water shortages. However, the analysis of overall climate change impacts was hindered by the differences between the models, including the way the surface water balance was calculated (lumped-parameter model or soil–vegetation–atmosphere scheme), or calibration and initialization methods. In addition, several regions of France had no available mode, such as the coastal Mediterranean region, the Rhône Valley, or Britany.

Several initiatives were taken to overcome the difficulty of providing a comprehensive modelling tool of French water resources, current strategies relying on gathering multiple independent models in the same numerical platform. Thus, the operational SAFRAN-ISBA-MODCOU (Système d'Analyse Fournissant des Renseignements Adaptés à la Nivologie–Interaction between Soil, Biosphere, and Atmosphere–MODèle COUplé; SIM) hydro-meteorological modelling chain was the first to build a national model based on two regional hydrogeological models (the Seine and Rhône River basins) within the same numerical tool (Habets *et al.* 2008). SIM provides operational forecasts of river flows and soil wetness for drought monitoring as well as climate change impact analysis over much of France (Dayon *et al.* 2018). Groundwater dynamics were included in SIM only for specific regions in the Rhône and Seine river basins, using a diffusivity equation (Rousset *et al.* 2004).

More recently, the AquiFR modelling platform has extended this approach by combining 13 regional groundwater models developed with two different modelling software programs (http://www.geosciences.ens.fr/aqui-fr/) (Vergnes *et al.* 2020). These models describe multilayer aquifer systems over more than 950 000 grid cells, with grid resolutions varying from 100 m to 1 km. They show a real benefit for drought forecasts and raised an expectation from stakeholders for consistent national groundwater forecasts at both seasonal-term (six months) and long-term (2050–2100) time scales. AquiFR takes advantage of previous modelling efforts and facilitates a multi-model analysis of the simulated hydrological variables, but limitations still remain, mainly due to the limited area covered by the existing models (about 30% of the French territory, corresponding mostly to sedimentary aquifer systems). Moreover, geometric and hydraulic inconsistencies

CONTACT Jean-Pierre Vergnes jp.vergnes@brgm.fr Water, Environment, Processes and Analyses Division, BRGM – French Geological Survey, Orléans 45060, France

remain at the boundaries of neighbouring regional models. Finally, the groundwater modelling software programs used for developing the various AquiFR models differ in their representation of hydrological processes and in their calibration strategies, which thus limit the consistency of the results.

Developing a single integrated large-scale hydrogeological model covering all of France would allow us to overcome these limitations. In the literature, the development of large-scale hydrogeological models has been given increasing attention over the last few decades (Fan *et al.* 2007, p. 200, 2013, Miguez-Macho *et al.* 2007, Gleeson *et al.* 2011, Vergnes and Decharme 2012, de Lange *et al.* 2014, Maxwell *et al.* 2015, de Graaf *et al.* 2017, Zeng *et al.* 2018). For example, de Graaf *et al.* (2017) developed a two-layer groundwater model at the global scale using a 5' grid cell resolution (about 10 km at the equator) in order to estimate global depletion of groundwater over the 1960–2010 period. Fan *et al.* (2013) simulates an equilibrium water table at the global scale at a 1 km resolution using a two-dimensional hydrogeological model. At the national scale, Westerhoff *et al.* (2018) adapted the model from the global study of Fan *et al.* (2013) to simulate an equilibrium water table state in New Zealand at a 200 m grid cell resolution. Over the United States, Maxwell *et al.* (2015) developed a more sophisticated three-dimensional high spatial resolution groundwater model (1 km grid), attempting to develop a parallel, integrated hydrologic model at a continental scale. They computed an equilibrium water table over a grid of about 30 million cells, but with the drawback of high computational time.

Over France, Vergnes *et al.* (2012) developed a simple groundwater scheme coupled to a land surface model for improving the simulation of climate in earth system models. Groundwater was represented with only a single layer at a resolution of about 10 km (1/12°) over the main sedimentary aquifer basins. The definition of geomorphological river and aquifer properties (geometries and hydrodynamic parameters) used a digital elevation model (DEM) data and simplified hydrogeological, lithological and geological maps available at the scale of France. Introducing groundwater improves the simulation of river flow to the sea. Besides, the water table feedback in the upper soil of the land-surface model increased evapotranspiration and thus impacted the lower boundary conditions of the atmospheric model (Vergnes *et al.* 2014). Despite the lack of many hydrological processes, including multilayer aquifer systems, groundwater withdrawal, and groundwater overflow, or the possibility of using nested model grids for refining a zone of interest, such as a groundwater pumping field or an area with river–aquifer exchanges, the results were promising and supported further improvement of the model.

However, using large-scale hydrological models as a reliable tool for decision making remains a challenge that must be overcome. The main objective of the present study is to demonstrate the feasibility of such a tool for assessing the impact of climate change on the French water resources. To fulfil this objective, the methodology developed by Vergnes and Decharme (2012) was augmented with the Modelling Aquifers with Rectangular cells, Transport and Hydrodynamics (MARTHE) computer code (Thiéry *et al.* 2020) at the finer resolution of 2 km. The model was evaluated against water table and river flow observations over a 10-year period, using the SAFRAN meteorological reanalysis. The surface-water budget was computed with a method based on the effective rainfall infiltration ratio (EPIR) (Lanini *et al.* 2019, Caballero *et al.* 2022). The impact of climate change on hydrological variables was then assessed using a set of regionalized climate projections available for France from the new DRIAS-2020 (Soubeyroux et al., 2021) climate database (http://www.drias-climat.fr).

2 Model and parameterizations

The new nation-wide spatially distributed model developed for France and presented here is based on the main parameterization aspects of Vergnes *et al.* (2012). It uses a 2 km grid cell resolution, finer than the 1/12° (about 10 km) resolution of the original model in Vergnes *et al.* (2012). It runs at weekly time steps for computing the hydrodynamics controlling the temporal evolution of groundwater levels and river flows. We selected a 2 km resolution and weekly time steps in order to limit the computational burden to a couple of hours of run time for the first version of the model. The model was developed with the MARTHE computer code and the surface-water budget was estimated using a lumped-parameter modelling method based on Edijatno and Michel (1989).

2.1 The MARTHE computer code

The MARTHE computer code (Thiéry *et al.* 2018, 2020) is a hydrogeological modelling software program developed by the French Geological Survey (BRGM). The basic concepts and equations of MARTHE are described in Thiéry *et al.* (2020) and are summarized in Appendix A. MARTHE embeds single-layer to multilayer aquifers and hydrographic networks; it is designed for two- or three-dimensional modelling of flow and mass transfer in aquifer systems, including climatic and human influences, and possible geochemical reactions. MARTHE considers the simulation of these physical processes in an integrated way that is particularly relevant for the modelling of hydrosytems at the regional or national scale. A free version of the numerical code is available on the BRGM web site (http://marthe.brgm.fr).

2.2 The surface-water budget

MARTHE requires a groundwater-recharge input for computing river flow and groundwater evolution. Recharge is derived by separating simulated effective rainfall into runoff and potential recharge. For evaluation of the model, the daily effective rainfall is estimated through a lumped-parameter modelling method based on Edijatno and Michel (1989). For the climate impact study, the daily effective rainfall is the mean of three water-budget methods that vary in how they calculate actual evapotranspiration and soil water storage (Thornthwaite 1948, Edijatno and Michel 1989, Dingman 1994). The distribution between potential groundwater recharge and surface runoff is carried out by multiplying the effective rainfall by EPIR (Lanini and Caballero 2016, Lanini *et al.* 2019). Further details on the computation of EPIR can be found in Appendix B.

2.3 Dataset and parameterization

Construction and parameterization of the river network model at the country scale requires the use of a DEM. We use the GMTED2010 DEM (Danielson and Gesch 2011) for computing the drainage direction in each grid cell, using GIS (Geographic Information System) processing, corresponding to the "r.watershed" command of the GRASS (Geographic Resources Analysis Support System) GIS (GRASS Development Team 2020). This creates a drainage-direction grid for integrating the river basins and tributaries into the model.

The hydrodynamic characteristics and definition of the aquifer transmissivity and porosity were taken from Vergnes *et al.* (2012) based on the simplified lithological map of France (BRGM; http://infoterre.brgm.fr).

More details about the parameterization of river networks, aquifer characteristics and river–groundwater exchanges can be found in Appendix C.

2.4 Model evaluation

A first simulation served to evaluate the model results against a set of observations over the 10-year period from 1 August 2000 to 31 July 2010.

2.4.1 Dataset evaluation

The SAFRAN meteorological forcing analysis dataset is a mesoscale atmospheric analysis system for surface variables (Vidal *et al.* 2010). It provides data on observed precipitation, 2 m air temperature, snow height and potential evapotranspiration flux for an 8 km resolution grid at a daily time step over France for computing effective rainfall.

In order to simplify the input data for this first model assessment, the EPIR map initially conceived at the hydrogeological unit scale was projected onto the SAFRAN grid to generate an EPIR coefficient for each cell of the 8 km grid.

For testing the model's sensitivity to the choice of meteorological input, a second simulation used the E-OBS meteorological dataset over the same evaluation period. E-OBS is a temperature and precipitation dataset covering Europe at a grid resolution of 0.25° (Cornes *et al.* 2018), based on the interpolation of station-derived meteorological observations available at the European scale. The same lumped-parameter method as the one using SAFRAN data was used to estimate the effective rainfall.

The evaluation concerns the evolution of the simulated groundwater levels for 66 piezometers chosen from the "Accès aux Données sur les Eaux Souterraines" (Access to groundwater data, ADES) database (Chery and Cattan (2003), http://www.ades.eaufrance.fr/). These piezometers are located in shallow groundwater aquifers with at least 5 years of daily data for the 10-year simulation period. The comparison between observed and simulated time series of river flow is carried out for four gauging stations located at the main river outlets of France (Fig. 1): the Seine at Poses (H811010), the Loire at Montjean (M5300010), the Garonne at La Magistère (O6140010), and the Rhône at Beaucaire (V7200010). The Hydro database (http://hydro.eaufrance.fr/) provides observed daily river flow data for of each of these gauging stations.

To evaluate the model, we compared the observed groundwater level and river flow datasets with simulated time series computed at weekly time steps.

2.4.2 Evaluation criteria

Statistical criteria were used to evaluate the simulation over the 10-year evaluation period. Bias B evaluates the deviation of mean simulated groundwater levels from the mean observed values for a specific piezometer. The coefficient of determination (R^2) compares the quality of fit of the simulation with observed time series of groundwater levels and river flows. The annual river flow ratio criterion (R_d) is defined as the mean annual simulated river flow divided by the mean annual observed river flow.

The Nash-Sutcliffe model efficiency coefficient E_f (Nash and Sutcliffe 1970) measures the variance between observed and simulated river flows, being 1 when the model perfectly fits the observations. An E_f criterion >0.7 is generally accepted as a good estimate of the signal dynamic, although this depends upon the hydrogeological and climate context of the basin. A negative E_f value means that the mean observed signal is a better predictor than the model.

The following normed root mean square error bias-excluded (E_{NRMSE_BE}) score (Vergnes *et al.* 2020) compares the observed and simulated groundwater levels:

$$E_{NRMSE\_BE} = \frac{1}{\sigma_{obs}} \sqrt{\frac{\sum_{t=1}^{n} \left[\left(H_{sim}(t) - \overline{H_{sim}} \right) - \left(H_{obs}(t) - \overline{H_{obs}} \right) \right]^2}{n}} \quad (1)$$

where $\overline{H_{sim}}$ is the temporal mean of simulated groundwater levels over the simulated period and σ_{obs} is the observed standard deviation. The E_{NRMSE_BE} criterion starts from 0 for a perfect simulation of the observed amplitudes and is always positive. An estimation of the temporal evolution of the observed water table can be considered reasonable for an E_{NRMSE_BE} criterion <0.8. Using the E_{NRMSE_BE} criterion rather than the RMSE score allows a better assessment of the amplitude and synchronization of the simulated time series, accounting for the differences in variability between the numerous wells to assist with spatial comparison or aggregation.

2.5 Climate change scenarios

The potential of the model as a tool for assessing climate change impact over France was explored using climate projections from the new DRIAS-2020 baseline climate projections (DRIAS 2021, http://www.drias-climat.fr/). In DRIAS-2020, 12 regionalized simulations from the Euro-CORDEX (CooRdinated Downscaling EXperiment - European Domain) ensemble (Jacob *et al.* 2020) were selected to form a set more easily usable for impact studies than the complete set that includes several hundred simulations. The present study used five regionalized climate projections from those available in DRIAS-2020, corresponding to the most pessimistic RCP (Representative Concentration Pathway) 8.5 radiative concentration pathway, leading to an increase of about 4°C in global mean temperature by the end of the century (van Vuuren *et al.*

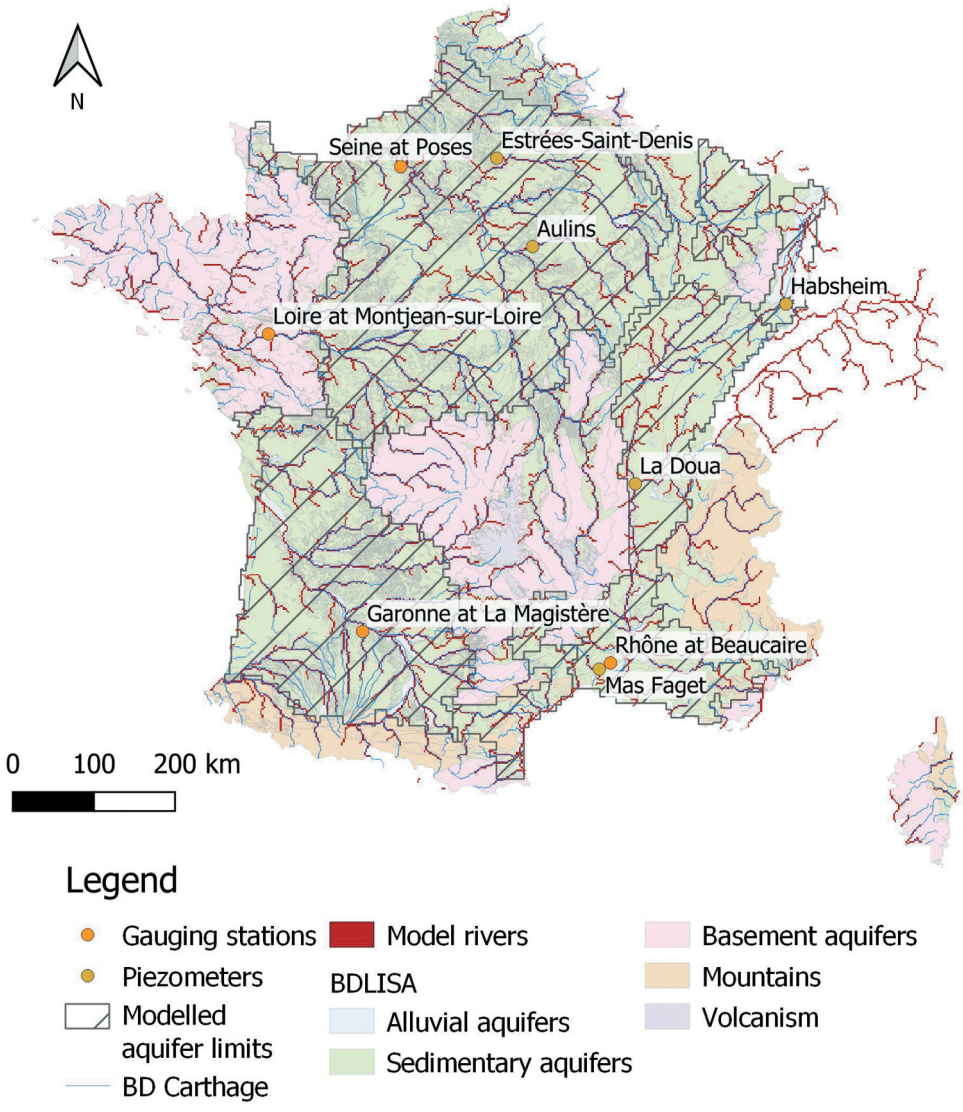

Figure 1. Aquifer limits from the Vergnes *et al.* (2012) model. The map background is from the French hydrogeological reference system *Base de Donnée des Limites des Systèmes Aquifères* (BDLISA; https://bdlisa.eaufrance.fr/). The locations of the corresponding piezometers and gauging stations of Fig. 3 and Fig. 4 are shown, as are the river network from Carthage Database (blue) and the model (red).

2011). These five projections were considered to be representative of the variability range of the 12 climate projections.

Two simulation periods were evaluated per climate model projection, the "present" historical period from 1 January 1976 to 31 December 2005 and the future period from 1 January 2070 to 31 December 2099. Daily time step climate projections were used for computing effective rainfall in both periods. Comparing simulated river discharges, river–groundwater exchanges, and groundwater levels between the two periods allows assessing the impact of climate change.

2.6 The standardized piezometric level index

In order to better assess the occurrence of future extreme events, a standardized piezometric level index (SPLI) was used. The SPLI is an indicator that compares groundwater level time series and characterizes the severity of extreme events such as a long dry period or groundwater overflow (Seguin 2015). It is currently used in France for the Monthly Hydrological Survey (MHS) (Office International de l'Eau 2019) and for the analysis of drought effects on groundwater (Vergnes *et al.* 2020).

The MHS provides monthly information on the hydrological state of groundwater. The SPLI is based on the same principles as the standardized precipitation index (SPI) defined by McKee *et al.* (1993) for defining meteorological drought at several time scales. First, monthly mean time series are computed from time series of piezometric heads. Then, 12 monthly time series (January to December) are constituted for the N years of the time series period. For each time series of N monthly values, a non-parametric kernel density estimator allows us to estimate the best probability density function fitting the histogram of monthly values. Finally, for each month from January to December, a projection of the standardized normal distribution using a quantile–quantile projection helps us deduce the SPLI for each value of the monthly mean time series of piezometric heads. The SPLI values are

Table 1. Classification of water table level classes related to the SPLI (Standardized Piezometric Level Index) values corresponding to MHS (Monthly Hydrological Survey) limits.

Classification	SPLI values	Return periods
Very low groundwater level	< −1.28	> 10 dry years
Low groundwater level	Between −1.28 and −0.84	Between 10 and 5 dry years
Moderately low groundwater level	Between −0.84 and −0.25	Between 5 and 2.5 dry years
Normal groundwater level	Between −0.25 and 0.25	Between 2.5 and 2.5 wet years
Moderately high groundwater level	Between 0.25 and 0.84	Between 2.5 and 5 wet years
High groundwater level	Between 0.84 and 1.28	Between 5 and 10 wet years
Very high groundwater level	> 1.28	> 10 wet years

normalized, ranging from −3 (extremely low groundwater levels during a return period of 740 years) to +3 (extremely high groundwater levels). The SPLI shows wetter and drier periods in a similar way throughout the simulated domain, and is categorized into seven classes from driest to wettest conditions (Table 1).

3 Results

3.1 Evaluation

3.1.1 Groundwater

Figure 2 shows the spatial distribution of B, R^2, and $E_{\mathrm{NRMSE\_BE}}$ scores computed for each of the 66 piezometers used for simulation with the SAFRAN meteorological dataset. B scores indicate that the model overestimates the simulated mean groundwater levels by more than 3 m for 56% of the piezometers and by more than 8 m for 41% of the piezometers. Conversely, the model underestimates the simulated mean groundwater levels by over −3 m for 25% of the piezometers without exceeding underestimation by −8 m.

Overestimations occur over the Paris Basin and in the New Aquitaine region. Underestimations particularly occur in the Rhine aquifer system and at the centre of the Paris Basin. R^2 scores are over 0.7 and 0.5 for 20% and 44% of the piezometers, respectively. Lower scores are found in the centre of the Paris Basin and north of the Rhine aquifer system. Finally, $E_{\mathrm{NRMSE\_BE}}$ scores corroborate the previous results with lower scores over the centre of the Paris Basin and the northern Rhine, while better scores are found in the New Aquitaine region as well as over the northeastern part of the Paris Basin.

The right-hand column of Fig. 2 shows the difference of absolute biases, R^2, and $E_{\mathrm{NRMSE\_BE}}$ scores between the simulations carried out with E-OBS and SAFRAN. For each map, red colours indicate an improvement and blue colours a degradation. Overall, E-OBS data seem to improve the bias scores (bias reduction) except for some piezometers located in the Paris Basin. R^2 scores are also improved over the centre of the Paris Basin while degradation occurs near the Poitou region. Finally, $E_{\mathrm{NRMSE\_BE}}$ shows contrasting results with better scores near the centre of the Paris Basin and lower scores over its western part. Elsewhere, no significant pattern appears, except a slight lowering of the scores over the Alsace plain.

Figure 3 compares the time series of simulated groundwater levels at weekly time steps with respect to observations from five piezometers (see Fig. 1) selected as representative of the results of the present evaluation. Table 2 presents the statistical scores associated with these comparisons, although the following comments only concern the SAFRAN simulation.

The piezometer located at Habsheim in the alluvial Rhine deposits shows good R^2 and $E_{\mathrm{NRMSE\_BE}}$ scores with a low bias score of −3.24 m. The piezometer located at Mas Faget in the alluvial deposits of the Vistrenque, near the Rhône outlet, provides another example of rather good agreement between observation and simulation, with a bias score of 1 m. The piezometers at Estrées-Saint-Denis and near Aulin are located in the chalk aquifer of the Paris Basin. Both present absolute biases of about 7 m, the groundwater levels of the first being overestimated and those from the second being underestimated. The Estrées-Saint-Denis piezometer shows good R^2 and $E_{\mathrm{NRMSE\_BE}}$ scores and the Aulin one poorer ones. The fifth piezometer is located in alluvial deposits of the Rhône River; it has a lower bias of 1 m with, however, R^2 and $E_{\mathrm{NRMSE\_BE}}$ scores of 0.59 and 1.09, respectively.

For the E-OBS simulation, bias scores show improvements for three of the five piezometers, except the Aulins and Habsheim ones, while R^2 and $E_{\mathrm{NRMSE\_BE}}$ scores are lower except for the Estrées-Saint-Denis piezometer.

3.1.2 River flows

Figure 4 compares the observed and simulated time series of river flow at the gauging stations on the Seine, Loire, Garonne and Rhône rivers (Fig. 1 and Table 3). For the SAFRAN simulation, all E_{f} scores are over 0.7. However, R_d scores are over 1 for the Seine (1.56) and Loire (1.26) rivers, in contrast to the good ratio scores of the Garonne (1) and Rhône (0.96) rivers. The model particularly overestimates the amplitudes of winter peaks for Seine and Loire. Overestimated R_{d} scores could be explained by deficiencies in the definition of the river network or in the computation of effective rainfall, as discussed in the next section.

For the E-OBS simulation, E_{f} scores are better for the Seine and Loire rivers, slightly lower (0.89 instead of 0.92) for the Rhône, and the same for the Garonne (0.92 for both simulations). While E_{f} scores remains good regardless of the simulation, E-OBS R_{d} scores are lower for the Rhône (0.67 instead of 0.96 for the SAFRAN simulation), Garonne (0.56 instead of 1), and Loire (0.75 instead of 1.26) rivers. Conversely, the score for Seine is 1.04. Lower scores at the Garonne, Rhône and Loire outlets indicate an underestimated effective rainfall computed with E-OBS. The almost-perfect value of 1.04 for the R_{d} score at the Seine outlet seems to indicate a compensation of errors due to deficiencies in the model structure rather than a better estimation of the effective rainfall from E-OBS.

3.2 Climate change impact

3.2.1 Impact on recharge

Figure 5 shows the relative changes of annual and seasonal mean potential groundwater recharge between future and past 30-year periods over France. Values are computed over the SAFRAN grid. Rows correspond to annual and seasonal means calculated for the December–January–February (DJF, winter), March–

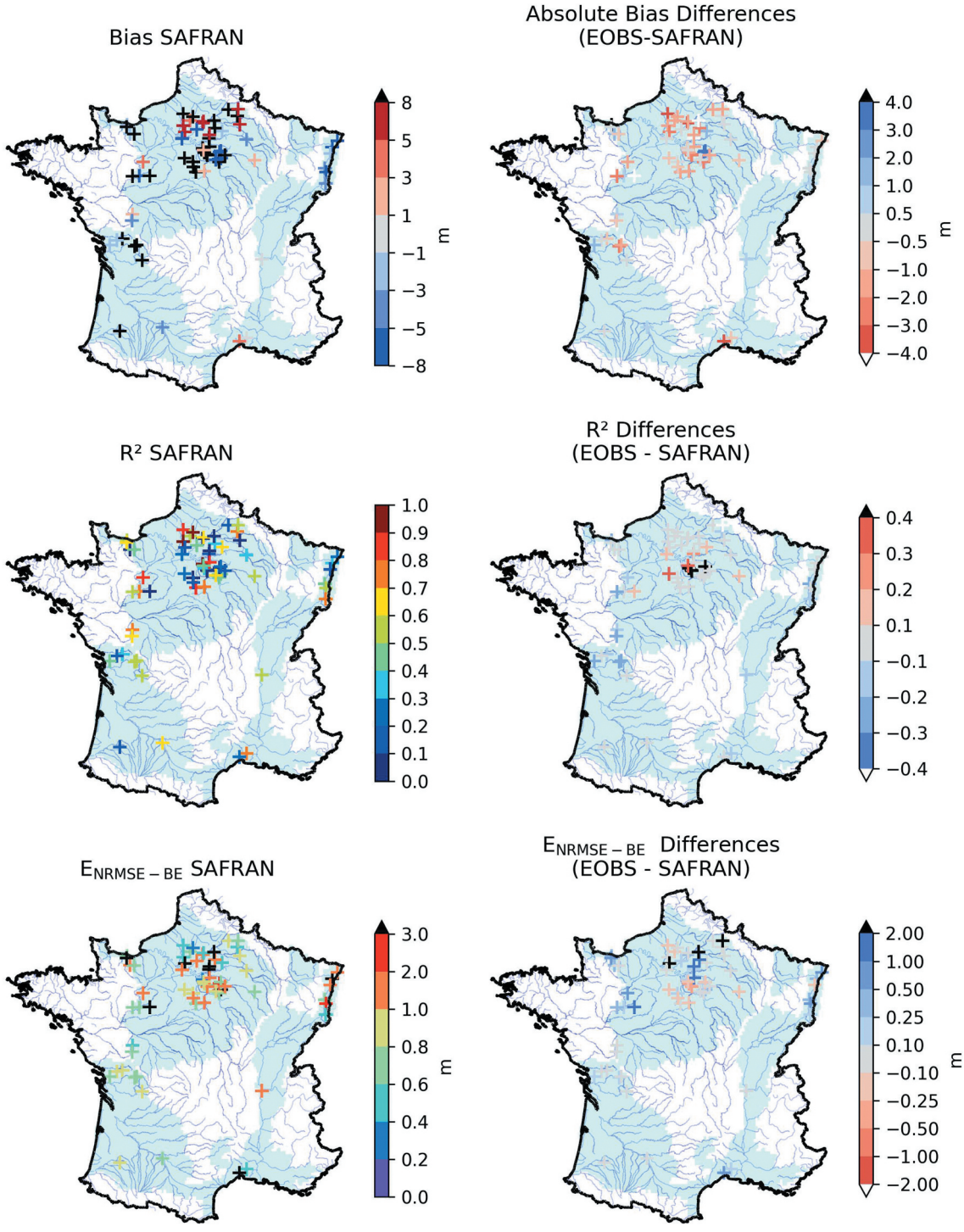

Figure 2. Left column: *B*, R^2 and E_{NRMSE_BE} scores computed for the 66 selected piezometers over the 10-year evaluation period using SAFRAN (Système d'Analyse Fournissant des Renseignements Adaptés à la Nivologie) data. Right column: differences of absolute bias, R^2 and E_{NRMSE_BE} scores between SAFRAN and E-OBS simulations. The blue shaded area is the simulated groundwater domain.

April–May (MAM, spring), June–July–August (JJA, summer), and September–October–November (SON, autumn) periods. Columns correspond to the ensemble minimum (most pessimistic), mean and maximum (most optimistic) of relative changes in annual and seasonal groundwater recharge among the five climate change simulations. Table 4 shows the ensemble minimum, mean, and maximum values for annual and seasonal changes spatially averaged over France. The selected climate projection sets lead to a future annual mean recharge increase of 15.3% over France. The most pessimistic scenario (ensemble minimum) projects a decrease of −3.3% and the most optimistic one an increase of 41.2%. The spatial distribution of the annual mean recharge splits the French territory into a northern wetter part and a southern drier part.

According to the ensemble mean, in winter, average groundwater recharge in winter would increase by 27.7%

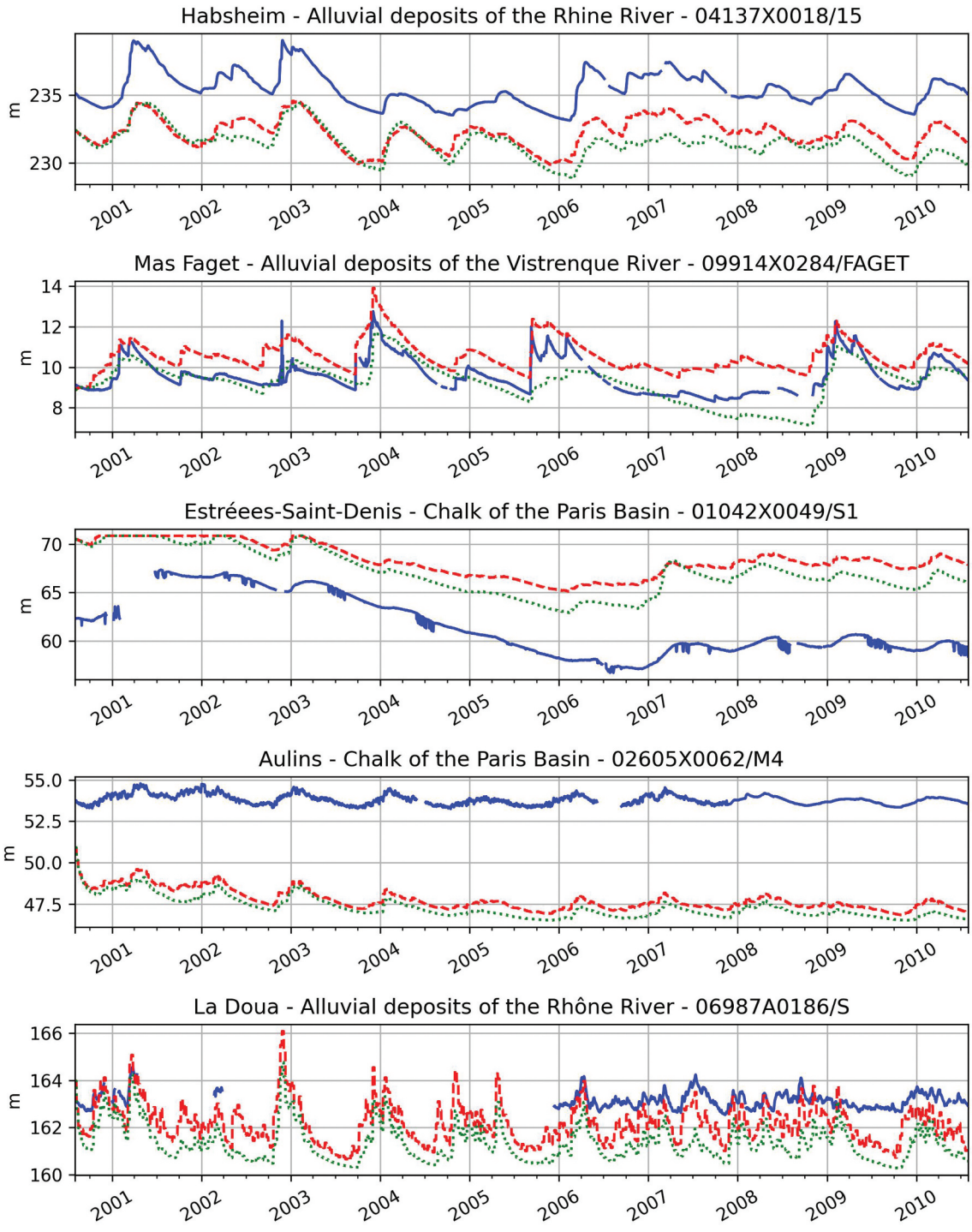

Figure 3. Simulated (dashed red for SAFRAN (Système d'Analyse Fournissant des Renseignements Adaptés à la Nivologie) and dotted green for E-OBS) and observed (solid blue) water table evolutions for the five selected piezometers in Fig. 1.

over France and decrease by 17% in summer. Wetter conditions in winter would concern almost all of the country while drier conditions in summer would be south of a northwest/southeast diagonal. The wetter scenarios (ensemble maximum) project a + 50% increase of the mean spatial recharge in winter throughout the country, reaching about 73% in summer (JJA) and autumn (SON). Conversely, the drier scenarios project mean spatial recharge decreases by −65% and −41%, respectively, in summer and autumn, again throughout the country. These results show the strong dispersion of climate scenarios in summer and fall.

3.2.2 Impact on water table levels

Similarly, Fig. 6 shows the difference in simulated water table levels between future and historical period, presenting annual and seasonal means. The ensemble mean projects water table level increases over the northern part of France, while decreases should affect the Mediterranean coast and the Pyrenees

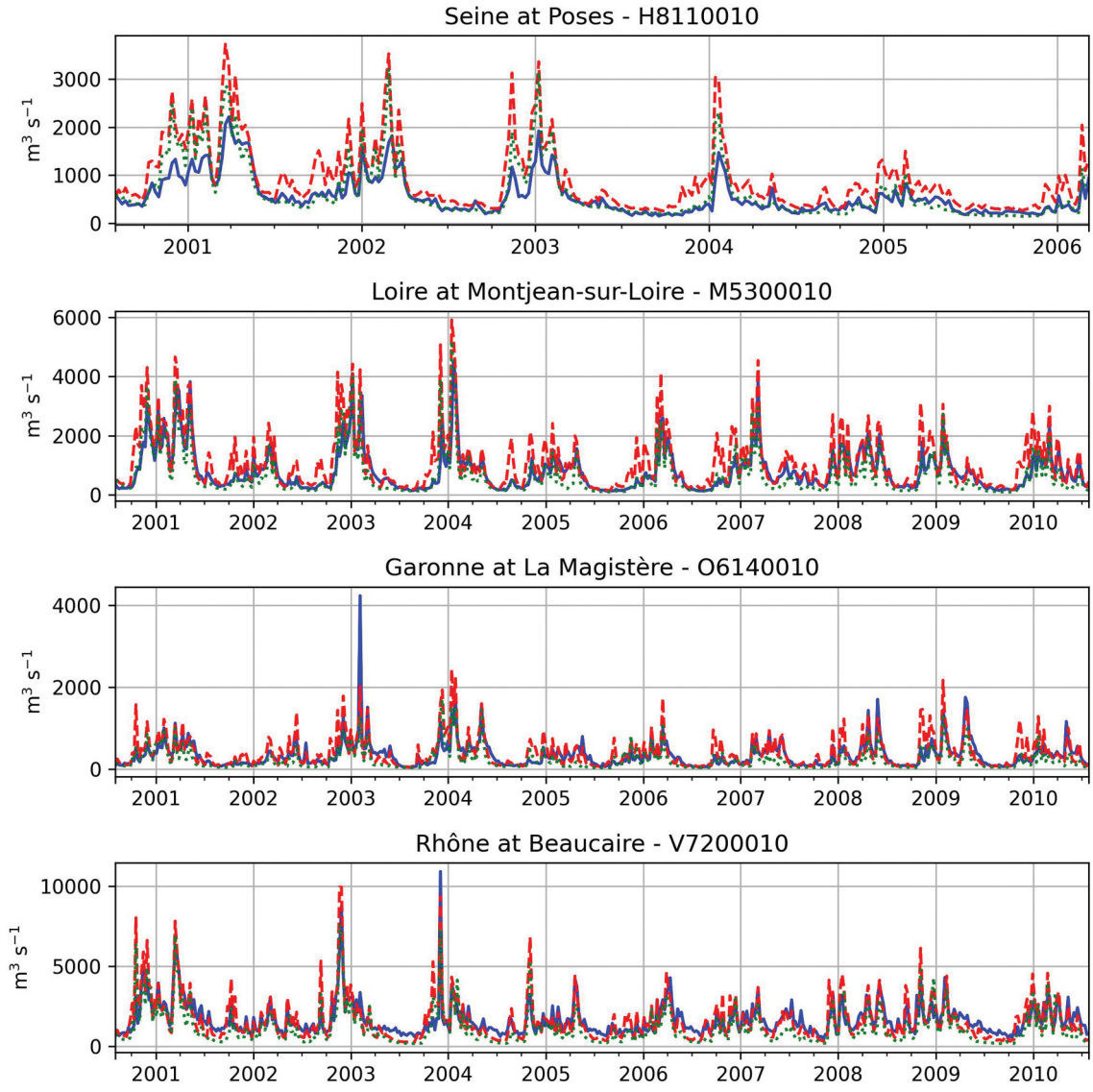

Figure 4. Simulated (dashed red for SAFRAN (Système d'Analyse Fournissant des Renseignements Adaptés à la Nivologie) and dotted green for E-OBS) and observed (solid blue) river flows at the four gauging stations in Fig. 1.

Table 2. Statistical scores between observed and simulated groundwater levels for the observation wells of Fig. 1, and for the two simulations based on SAFRAN (Système d'Analyse Fournissant des Renseignements Adaptés à la Nivologie) and E-OBS meteorological datasets, respectively.

		SAFRAN	E-OBS
Habsheim	R^2	0.78	0.6
	E_{NRMSE_BE}	0.47	0.65
	B	−3.24	−3.98
Mas Faget	R^2	0.76	0.59
	E_{NRMSE_BE}	0.47	0.68
	B	0.99	−0.24
Estrées-Saint-Denis	R^2	0.70	0.72
	E_{NRMSE_BE}	0.59	0.52
	B	6.78	5.53
Aulins	R^2	0.48	0.35
	E_{NRMSE_BE}	1.56	1.76
	B	−6.04	−6.51
La Doua	R^2	0.59	0.4
	E_{NRMSE_BE}	1.08	1.15
	B	−0.93	−1.78

Table 3. R_d and E_f scores between observed and simulated river discharges for the gauging stations in Fig. 1.

		SAFRAN	E-OBS
Seine at Poses	R_d	1.56	1.04
	E_f	0.7	0.91
Loire at Montjean	R_d	1.26	0.75
	E_f	0.92	0.96
Garonne at La Magistère	R_d	1	0.56
	E_f	0.92	0.92
Rhône at Beaucaire	R_d	0.96	0.67
	E_f	0.92	0.89

Mountains. The driest projections (ensemble minimum) would lead to lower water table levels over the northern part of the Paris Basin, in the Aquitaine Basin, and in the Rhône Valley. Conversely, the wettest projections would result in higher water table levels over most of the country, except for some grid cells in the extreme south. Seasonal results show similar patterns, with a more intense lowering of groundwater levels in summer and autumn.

In order to assess the evolution of extreme events in the future, we computed the SPLI over each grid cell of the simulated groundwater domain for the historical and future 30-year periods. The reference period for the computation of

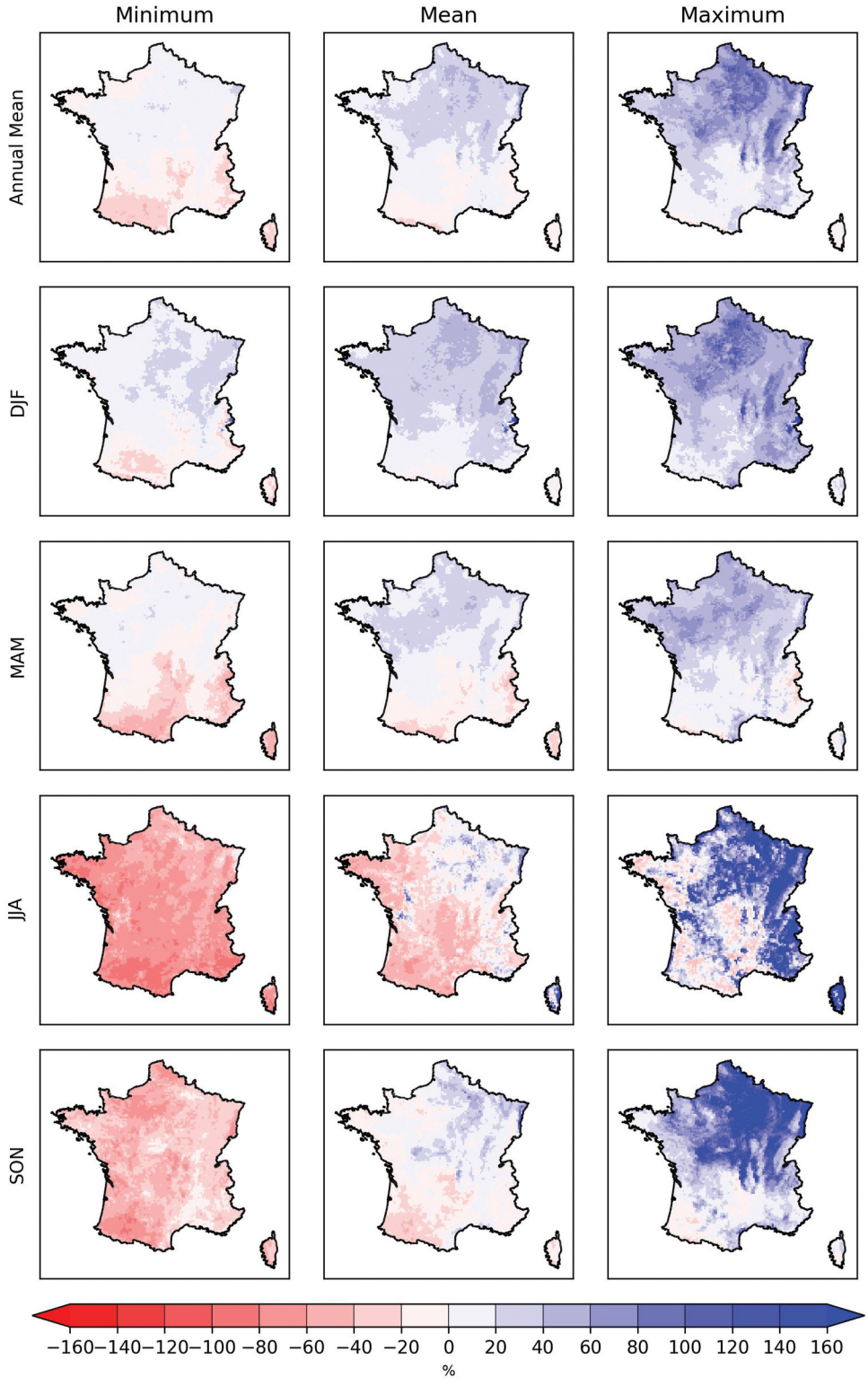

Figure 5. Future spatial distribution of relative groundwater recharge evolution compared to the historical period over France, calculated on the SAFRAN (Système d'Analyse Fournissant des Renseignements Adaptés à la Nivologie) grid. Columns correspond to the ensemble minimum (drier simulations), mean, and maximum (wetter simulations) recharge estimations. Rows correspond to the annual mean and the seasonal means for December–January–February (DJF), March–April–May (MAM), June–July–August (JJA) and September–October–November (SON).

the SPLI is the 1976–2005 historical period for both the historical and future periods. The percentages of monthly SPLI values belonging to each category of Table 1 were computed for both 30-year periods (present and future) over each grid cell. Figure 7 shows the ensemble mean values of these percentages, spatially aggregated over the simulated domain. Error bars correspond to spatially aggregated ensemble minimum and maximum values. Normal

Table 4. Variation (5) of the spatial mean recharge between the future and the reference period for the annual and seasonal means. Ensemble minimum, mean and maximum values are shown.

	Annual mean	DJF	MAM	JJA	SON
Ensemble minimum (%)	−3.3	+8.5	−8.9	−64.9	−41
Ensemble mean (%)	+15.3	+27.4	+9.1	−17.1	2.1
Ensemble maximum (%)	+41.2	+50.5	+29.2	+73	73.8

occurrences diminish in the future by about 5%. Future occurrences of wettest events increase to the detriment of driest events. Very high groundwater level events increase by about 10% with respect to the reference period, while events with very low groundwater levels remain close to 5%. The more extreme the events are, the greater will be the dispersion of projections, especially for the very high groundwater level category. However, all projections agree on a future increase of wettest conditions.

For each grid cell, the percentages of monthly SPLI values belonging to "very low groundwater level" and "very high groundwater level" were calculated for both historical and future periods. Figure 8 shows the differences in these percentages between future and historical periods for these two SPLI categories. Blue colours correspond to wetter conditions, meaning negative (positive) trends of very low (high) groundwater levels in the future compared to the present. Red corresponds to drier conditions. Columns represent ensemble minimum, mean and maximum values computed from the five climate projections.

Regarding the evolution of very low groundwater levels, the ensemble means show an increase of the driest conditions over the southern Aquitaine Basin. Ensemble maxima (driest projections) confirm this pattern, also leading to drier conditions in the northern part of the Paris Basin. Conversely, no drier conditions are projected for the ensemble minima (wettest projections).

Concerning the impact on the very high groundwater level category, the entire Paris Basin, the north of the Aquitaine Basin and the north of the Rhône Valley would experience increased wet conditions in the future. The ensemble maximum (wetter projections) shows wetter conditions for the entire simulated domain. The ensemble minimum (drier projections) would present fewer occurrences of wet events in the Aquitaine Basin and in the northwestern part of the Paris Basin, but an increase of wetter events would still dominate in the Paris Basin.

3.2.3 Impact on river–groundwater exchanges

In addition to the previous results, Fig. 9(a) shows the spatial distribution of the annual mean river–groundwater exchanges over the historical period for the ensemble mean climate projections. Losing rivers correspond to negative fluxes and gaining rivers to positive fluxes. Over the historical period, gaining rivers prevail over France. Thus, the spatial mean of river–groundwater exchanges computed for the entire river network is equal to +0.11 m^3/s from the aquifers to the rivers.

Figure 9(b) shows the relative changes in the annual mean river–groundwater exchanges between the future and the present period for the ensemble mean climate projections. Positive changes in the future mean more water available in the rivers, through either increases of river gains or decreases of river losses. Positive changes occur over the Paris Basin, the Rhône Valley and the north of the Aquitaine Basin, while negative changes occur over the southern Aquitaine Basin. The spatial mean value of river–groundwater exchanges changes is equal to +9% over France. However, only 0.6% of the grid cells switch from losing to gaining rivers from the present to the future periods, meaning that future conditions could be roughly stationary in terms of flow directions between river and groundwater.

3.2.4 Impact on river flow

Figure 10(a) shows the monthly mean seasonal cycle of simulated river flow at the four gauging stations (in Fig. 1) for the historical and future periods. Figure 10(b) shows the monthly mean seasonal cycle of simulated future river flow changes relative to the historical period. The envelope represents the simulated dispersion between minimum and maximum values. The mean simulated river flow in the Seine, Loire and Rhône rivers would increase during winter and decrease the rest of the year. Maximum decrease would occur during autumn, with a peak of −40% in September for the Loire. The mean simulated river flow in the Garonne River would increase for most of the year.

4 Discussion

The modelling method presented in this paper proves the feasibility of building a groundwater model that includes the simulation of river flows at the scale of France. While the earlier national initiatives within the AquiFR project (Vergnes *et al.* 2020) or the SIM platform (Habets *et al.* 2008, Le Moigne *et al.* 2020) relied on existing groundwater models built with different numerical codes, using a national hydrogeological model developed with the same computer code has several advantages. First, there is no need to deal with boundary conditions between models that can create multiple problems in a multi-model setup, such as which model to retain in case of model superimposition, or inconsistencies between the model geometries, or technical issues linked to the use of multiple numerical codes, such as if groundwater fluxes needs to be exchanged between models. It also eases the analysis and exploitation of the simulated results, and allows simulating groundwater changes in regions not covered by hydrogeological models, such as the southern part of the Rhône River basin.

The results of the present climate impact study agree with the DRIAS-2020 report (DRIAS, 2021, only available in French). Spatial patterns found for the relative changes of

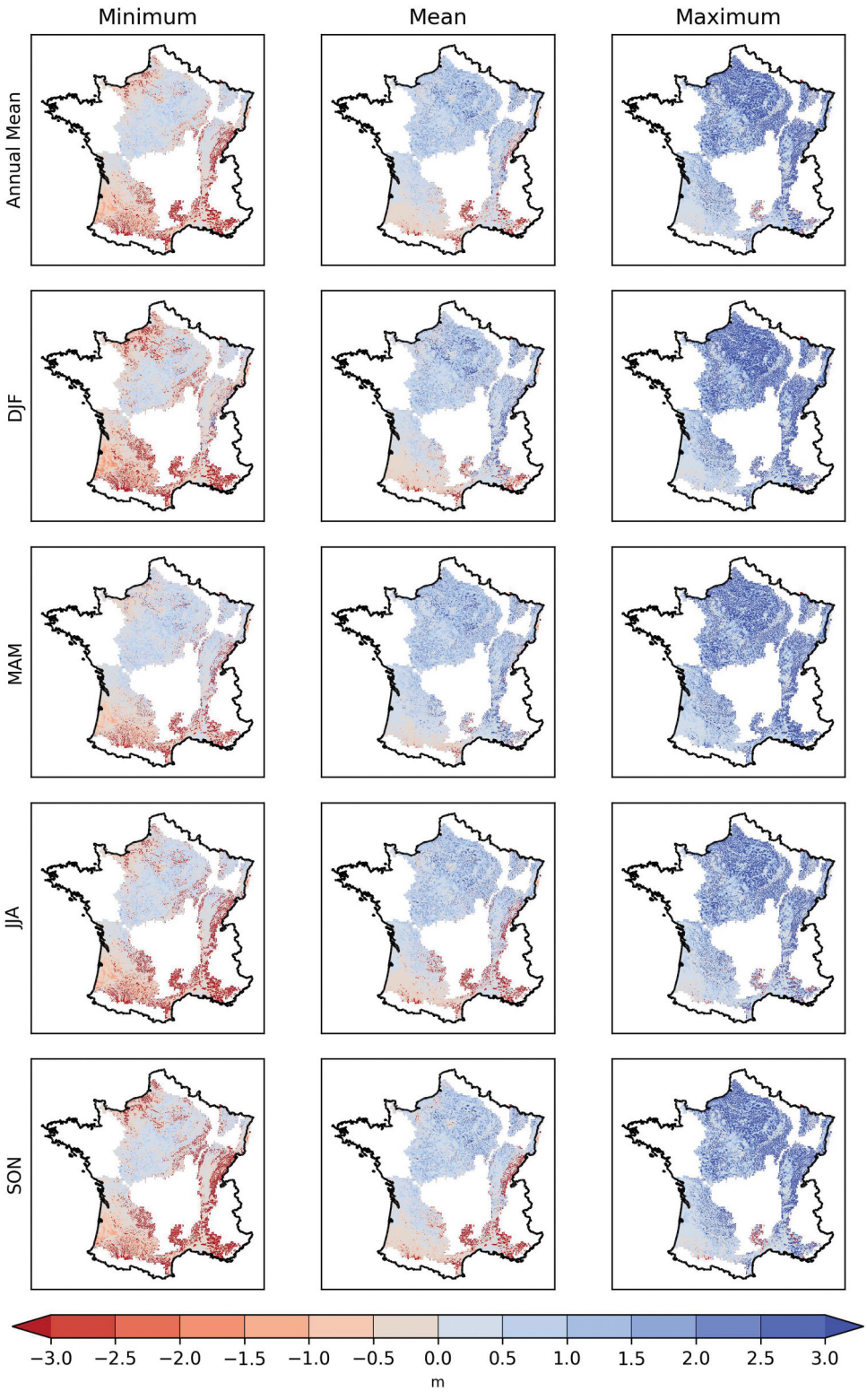

Figure 6. Annual and seasonal differences between future and historical simulated annual mean water table levels, in metres, for the ensemble minimum, mean, and maximum climate projections.

future groundwater recharge agree with projected increases in precipitation of the RCP 8.5 scenario for the 2070–2099 period over much of the French territory. In addition, the present study also projects higher groundwater levels on average over France in the future.

These results are quite different from those of previous climate change impact studies (Caballero *et al.* 2007, Stollsteiner 2012, Chauveau *et al.* 2013, Dayon *et al.* 2018, Wunsch *et al.* 2022). Wunsch *et al.* (2022) applied a neural network method over Germany to simulate groundwater level

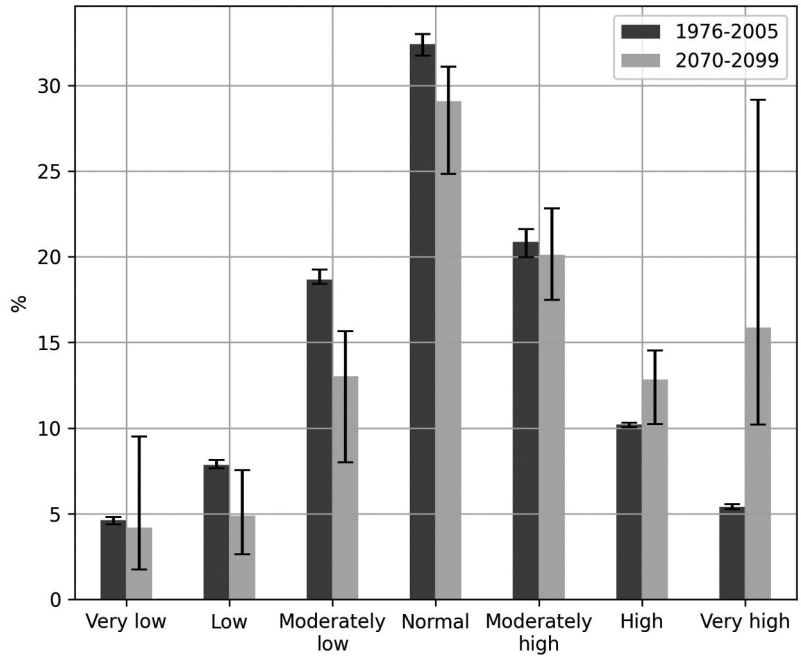

Figure 7. Mean spatial aggregation of monthly SPLI (Standardized Piezometric Level Index) values computed for each grid cell. Each category of Table 1 is shown for the historical and future periods. Greyscale bars correspond to the ensemble means while error bars correspond to the ensemble minima and maxima.

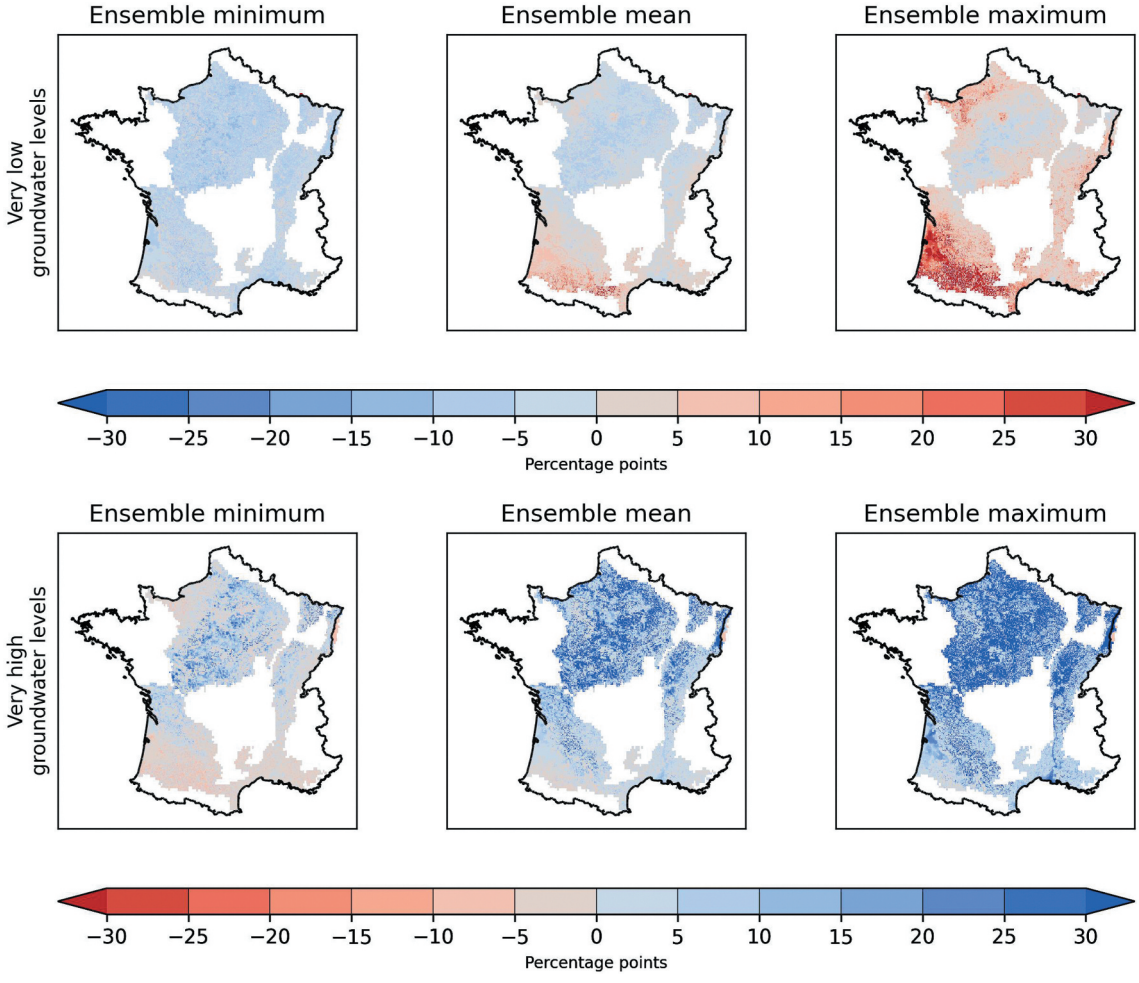

Figure 8. Spatial distribution of very low and very high groundwater level SPLI (Standardized Piezometric Level Index) categories in terms of percentage points between the future and historical periods. Blue colours correspond to wetter conditions and negative (positive) trends of very low (high) groundwater levels categories in the future compared to the present. In a similar way, red colours correspond to drier conditions.

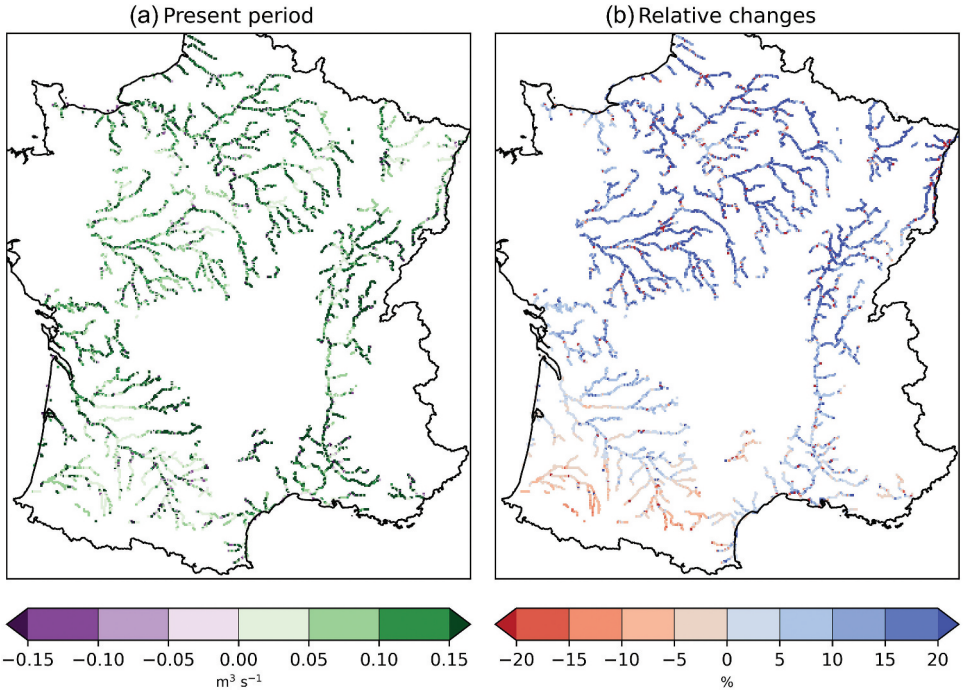

Figure 9. (a) Spatial distribution of the annual mean river–groundwater exchanges over the historical period for the ensemble mean climate projections. (b) Spatial distribution of the relative changes of the annual mean river–groundwater exchanges between the future and the present period for the ensemble mean climate projections.

evolution under climate change. Their results show a median relative change of groundwater levels ranging from −18% to −6% between 2014 and 2100 depending upon the projection, leading to an opposite trend compared with our results. In France, the Explore 2070 study projected lower recharge and groundwater levels over France by 2070. It was based on climate projections from the CMIP4 (Climate Model Intercomparison Project 4) global climate models (GCMs) downscaled with a statistical method by weather type (Boé *et al.* 2006, Chauveau *et al.* 2013). Dayon *et al.* (2018) found similar trends over France by using more recent climate projections from CMIP5 (Taylor *et al.* 2012) downscaled with a statistical method (Dayon *et al.* 2015).

The DRIAS-2020 set also uses the CMIP5 GCM projections (Terray and Boé 2013), downscaled with dynamical methods based on regional climate models (Jacob *et al.* 2014) and bias-corrected with a new statistical quantile–quantile method (Verfaillie *et al.* 2017). However, DRIAS-2020 projects wetter conditions for the future compared to the earlier regionalized climate projections for France, which may indicate inconsistencies in the climate projections, in both time and space (Dayon *et al.* 2018), that are mainly due to differences in the methods used for generating and regionalizing climate projections across studies. While exceeding the scope of the present study, a more thorough comparison of these differences is required for understanding their impact on simulating future hydrological variables.

The 10-year historical evaluation based on meteorological data from SAFRAN reveals some limitations of the modelling method. A comparison between the river networks built for the model and those of the BD Carthage database for France shows inconsistencies in the modelled river network (Fig. 1), which refer to missing or wrong paths of the network or its connections. They could be due to uncertainties associated with the DEM used for the modelled river network, to errors arising from the 2 km resolution of the model, or to structural uncertainties linked to the GIS algorithm used for computing the river tributaries and watershed areas. These inconsistencies could be responsible for overestimating the ratio scores when evaluating the simulated river flows, thus leading to misinterpretation of the available future water volumes, for example during low flow in summer.

Surface and groundwater withdrawals for human activities and hydraulic infrastructures (dams, channels, etc.) were not considered in the model, although numerous dams affect the flows of the Rhône and Garonne rivers. The Seine River flow at Poses is influenced by four large storage reservoirs used for flood control and located upstream in the watershed. Inclusion of water withdrawals and hydraulic infrastructures in the model needs a good knowledge of these data and their management strategies, which is not always available. Besides, the future evolution of such data is an unknown factor that is another source of uncertainty for long-term hydrological projections. Using the presented model without withdrawal for future projections provided a first assessment of the relative climate change impact on groundwater, but as yet does not provide operational information for groundwater management.

Comparison between simulations with the SAFRAN and E-OBS datasets shows that the sensitivity of effective rainfall computation to meteorological input is variable depending upon the geographic location. It is also sensitive to the water holding capacity of soils as can be estimated from the INRAE (National Research Institute for Agriculture, Food and

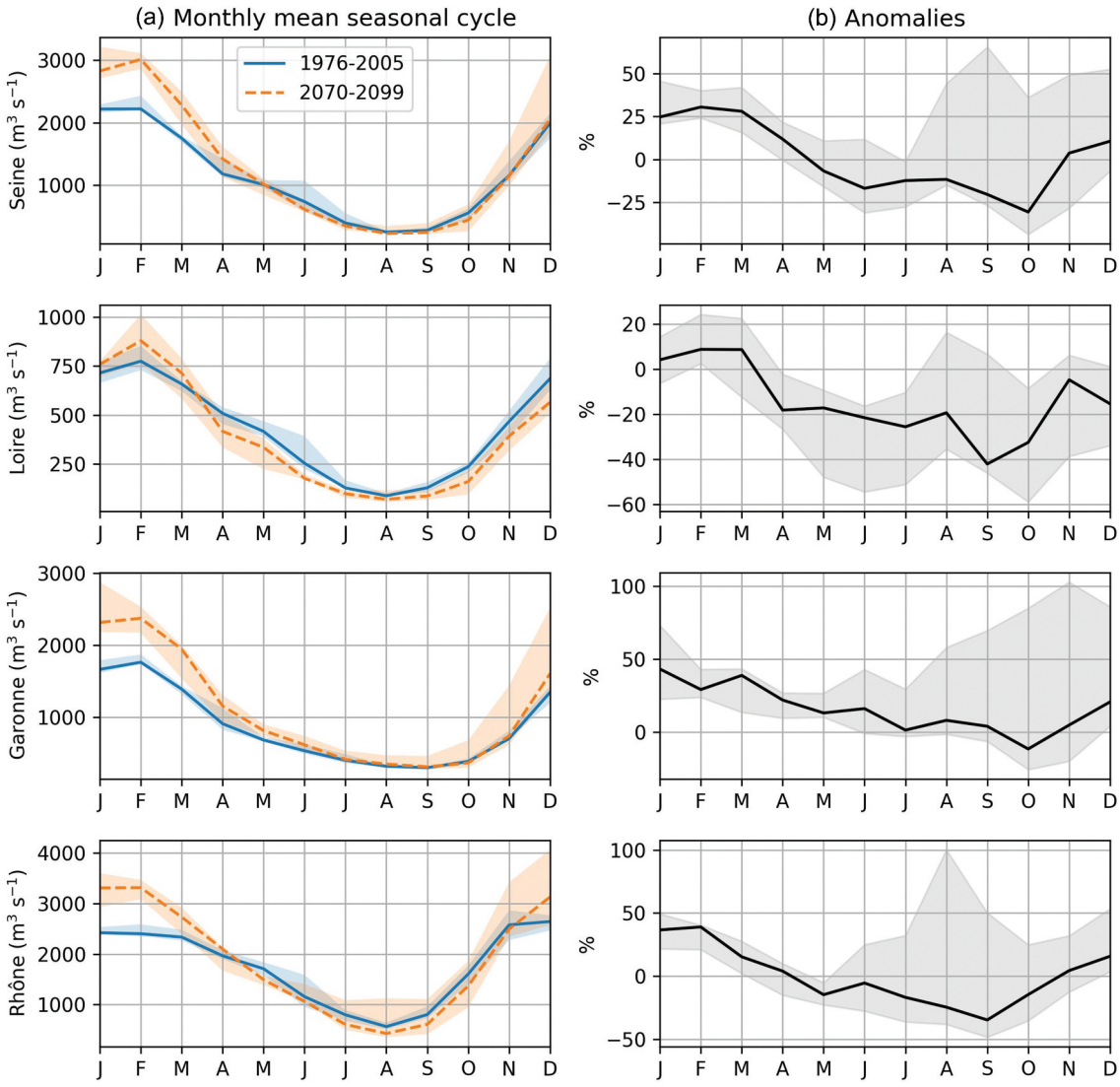

Figure 10. (a) Monthly mean seasonal cycles of the simulated river flow at the four selected gauging stations in Fig. 1 for the historical (solid blue) and future (dashed orange) periods. Bold lines correspond to ensemble means and shaded areas to ranges of the ensemble values. (b) Future anomalies of monthly mean river flow are shown in terms of relative change percentages with respect to the historical period. The bold line corresponds to the ensemble means, and shaded areas to value ranges between the ensemble minima and maxima.

Environment) soil map (Le Bas 2020), and to the land use effect on evaporation (Nistor *et al.* 2018), points not considered in our modelling method.

The EPIR estimate used for potential groundwater recharge computation is further subjected to uncertainties depending on location and considered geological characteristics, as well as on the baseflow separation method (Lanini *et al.* 2019). Besides, the computed groundwater recharge is provided as potential flow, but part of it may return to streams before reaching the aquifer. It may also not be stored in the aquifer, as aquifer storage capacities are not considered in the recharge computation method. Thus, by definition, the potential recharge we calculate is always greater than or equal to the actual recharge. As such, it could explain part of the overestimations of simulated groundwater levels for some piezometers associated with underestimated river flows. Systematic methods for estimating the actual recharge at the national scale have yet to be developed, and, once operational, may also be subject to significant uncertainties (Alcalá and Custodio 2014, Westerhoff *et al.* 2018).

The description of aquifer geometry and hydrodynamic characteristics at a national scale relies on coarse assumptions defined by Vergnes and Decharme (2012) for application in GCMs with coarse grid cell resolutions (about 0.5°), which might explain some of the inconsistencies in model evaluation. Groundwater evolution can be influenced by boundary conditions of the aquifers, either through vertical water exchange or through the spatial extent of recharge. Describing multilayer aquifer systems with a better delineation of their geometry could be done based on modern hydrogeological and geological databases, such as the French hydrogeological referential (BDLISA, https://bdlisa.eaufrance.fr/, Brugeron *et al.* 2018), the subsoil database (BSS, https://infoterre.brgm.fr/), or the French geological referential (RGF, http://rgf.brgm.fr/). The

inclusion of aquifers in basement areas could be considered as well, in view of the 2 km model resolution and the porous-like behaviour of superficial aquifers of basement rocks at this scale.

In addition, current aquifer parameters mostly are coarse estimates. Their uncertainties need better estimates as do their actual values, either using existing data (Gleeson *et al.* 2011) or using a semi-automatic calibration method, such as the PEST tool (Doherty and Hunt 2010). In addition, we might include ground- and surface water withdrawal data from the national pumping database (BNPE, https://bnpe.eaufrance.fr/). Finally, an enhanced evaluation of groundwater simulation could be planned using an appropriate set of piezometers little influenced by groundwater pumping (Baulon *et al.* 2020).

A 20-year simulation with a 2 km resolution regular grid and weekly time steps takes about 2 to 3 hours of simulation with MARTHE using a single-core processor run. Based on this estimate, adding new aquifer layers to represent multilayer aquifer systems would certainly increase this computation time although it would maintain a reasonable computational burden, limited to a couple of days in the worst case.

However, increasing the spatial resolution would require modification of the MARTHE computer code. Future development paths could include the parallelization of groundwater numerical schemes or the use of an unstructured grid in order to refine the zone of interest (such as near rivers or over pumping fields), while maintaining coarser resolution in other domains, such as in deep confined aquifers.

5 Conclusions

The modelling method presented in this paper shows a varying performance depending on the regions and variables considered, but provides encouraging results for a groundwater modelling exercise at the scale of France. We demonstrated the potential of constructing a groundwater model covering much of France with a spatial resolution of 2 km for providing insights into the impact of projected climate change scenarios. A selection of regionalized climate projections from the new DRIAS-2020 dataset, using the most pessimistic RCP 8.5 greenhouse gas scenario, projects the wettest conditions for France with increased recharge and higher groundwater levels, by the 2070–2099 period. Only the Mediterranean coast and the southern Aquitaine Basin would experience drier conditions with increased extreme dry events.

The method used here was originally developed for the ISBA-CTRIP (national Centre for meteorological research version of Total Runoff Integrating Pathways) hydrologic continental model (Vergnes and Decharme 2012, Decharme *et al.* 2019). Its direct integration into the MARTHE groundwater modelling tool is a successful demonstrator of the interest in building a more detailed hydrological model for France. The satisfactory results from using pan-European meteorological E-OBS data indicates that the vision of producing the same type of modelling method at a European scale is realistic.

Several improvements may lead to still more robust results, in particular a refined computing of the river networks, better descriptions of the aquifer geometry in the case of multilayer sedimentary aquifers, or inclusion of the basement rock areas of the Massif Central and Britany. It will also be necessary to recalibrate both river and aquifer parameters (not modifying them from the values provided by Vergnes and Decharme (2012)) and to include data on groundwater withdrawal.

Nonetheless, being a physically-based modelling tool of groundwater behaviour, the MARTHE model is an interesting tool for assessing the impact of climate change on ground and surface- water resources at a national scale. Such results would help groundwater managers in selecting among different adaptation strategies aimed at mitigating the effects of climate change, at least at a regional scale.

Acknowledgements

This work was supported by the INDECIS project, financed by the European ERA4CS Joint Call for Transnational Collaborative Research Projects. The authors thank one anonymous reviewer and R. Westerhoff and Associate Editor M. Bianchi for their useful reviews and comments that greatly improved this manuscript. H.M. Kluijver edited the final English manuscript for language and content.

Disclosure Statement

No potential conflict of interest was reported by the authors.

ORCID

Jean-Pierre Vergnes http://orcid.org/0000-0001-5659-0554
Yvan Caballero http://orcid.org/0000-0002-5328-7338
Sandra Lanini http://orcid.org/0000-0003-2471-4326

References

Alcalá, F.J. and Custodio, E., 2014. Spatial average aquifer recharge through atmospheric chloride mass balance and its uncertainty in continental Spain. *Hydrological Processes*, 28 (2), 218–236. doi:10.1002/hyp.9556.

Amanambu, A.C., et al., 2020. Groundwater system and climate change: present status and future considerations. *Journal of Hydrology*, 589, 125163.

Arora, V., et al., 2001. Scaling aspects of river flow routing. *Hydrological Processes*, 15 (3), 461–477. doi:10.1002/hyp.161.

Asch, K., 2005. *The 1: 5 million international geological map of Europe and adjacent areas-IGME 5000*. Hanover, Germany: Bundesanstalt für Geowissenschaften und Rohstoffe.

Baulon, L., et al., 2020. Influence de la variabilité basse-fréquence des niveaux piézométriques sur l'occurrence et l'amplitude des extrêmes. *Géologues* (207).

Boé, J., et al., 2006. A simple statistical-dynamical downscaling scheme based on weather types and conditional resampling. *Journal of Geophysical Research: Atmospheres*, 111 (D23). doi:10.1029/2005JD006889.

Brugeron, A., Paroissien, J.B., and Tillier, L., 2018. *Référentiel hydrogéologique BDLISA version 2 : principes de construction et évolutions. Rapport final*. Orléans, BRGM/RP-67489-FR, No. BRGM/RP-67489-FR.

Caballero, Y., et al., 2007. Hydrological sensitivity of the Adour-Garonne river basin to climate change. *Water Resources Research*, 43 (7). doi:10.1029/2005WR004192.

Caballero, Y., et al., 2022. Present and future potential groundwater recharge evaluation at the scale of France. *Submitted to Comptes Rendus Geoscience*.

Chauveau, M., et al., 2013. Quels impacts des changements climatiques sur les eaux de surface en France à l'horizon 2070 ? *La Houille Blanche*, 99 (4), 5–15. doi:10.1051/lhb/2013027.
Chery, L. and Cattan, A., 2003. ADES. National groundwater database. *La Houille Blanche*, 89 (2), 115–119. doi:10.1051/lhb/2003038.
Cornes, R.C., et al., 2018. An ensemble version of the E-OBS temperature and precipitation data sets. *Journal of Geophysical Research: Atmospheres*, 123 (17), 9391–9409. doi:10.1029/2017JD028200.
Crosbie, R.S., et al., 2013. Potential climate change effects on groundwater recharge in the high plains aquifer, USA. *Water Resources Research*, 49 (7), 3936–3951. doi:10.1002/wrcr.20292.
Cuthbert, M.O., et al., 2019. Global patterns and dynamics of climate–groundwater interactions. *Nature Climate Change*, 9 (2), 137–141. doi:10.1038/s41558-018-0386-4.
Danielson, J.J. and Gesch, D.B., 2011. Global multi-resolution terrain elevation data 2010 (GMTED2010): U.S. Geological Survey Open-File Report. No. 1073.
Dayon, G., et al., 2018. Impacts of climate change on the hydrological cycle over France and associated uncertainties. *Comptes Rendus Geoscience*, 350 (4), 141–153. doi:10.1016/j.crte.2018.03.001.
Dayon, G., Boé, J., and Martin, E., 2015. Transferability in the future climate of a statistical downscaling method for precipitation in France. *Journal of Geophysical Research: Atmospheres*, 120 (3), 1023–1043. doi:10.1002/2014JD022236.
Decharme, B., et al., 2010. Global evaluation of the ISBA-TRIP continental hydrological system. Part II: uncertainties in river routing simulation related to flow velocity and groundwater storage. *Journal of Hydrometeorology*, 11 (3), 601–617. doi:10.1175/2010JHM1212.1.
Decharme, B., et al., 2012. Global off-line evaluation of the ISBA-TRIP flood model. *Climate Dynamics*, 38 (7), 1389–1412. doi:10.1007/s00382-011-1054-9.
Decharme, B., et al., 2019. Recent changes in the ISBA-CTRIP land surface system for use in the CNRM-CM6 climate model and in global off-line hydrological applications. *Journal of Advances in Modeling Earth Systems*, 11 (5), 1207–1252. doi:10.1029/2018MS001545.
de Graaf, I.E.M., et al., 2017. A global-scale two-layer transient groundwater model: development and application to groundwater depletion. *Advances in Water Resources*, 102, 53–67. doi:10.1016/j.advwatres.2017.01.011
de Lange, W.J., et al., 2014. An operational, multi-scale, multi-model system for consensus-based, integrated water management and policy analysis: the Netherlands hydrological instrument. *Environmental Modelling & Software*, 59, 98–108. doi:10.1016/j.envsoft.2014.05.009
Dingman, S.L., 1994. *Physical hydrology*. New Jersey, USA: Prentice Hall Upper Saddle River.
Doherty, J.E. and Hunt, R.J., 2010. Approaches to highly parameterized inversion—A guide to using PEST for groundwater-model calibration. U.S. Geological Survey, No. U.S. Geological Survey Scientific Investigations Report 2010–5169.
Eakin, T.E., 1966. A regional interbasin groundwater system in the White River Area, southeastern Nevada. *Water Resources Research*, 2 (2), 251–271. doi:10.1029/WR002i002p00251.
Edijatno, and Michel, C., 1989. Un modèle pluie-débit journalier à trois paramètres. *La Houille Blanche*, 75 (2), 113–122. doi:10.1051/lhb/1989007.
Fan, Y., et al., 2007. Incorporating water table dynamics in climate modeling: 1. Water table observations and equilibrium water table simulations. *Journal of Geophysical Research*, 112 (D10), D10125. doi:10.1029/2006JD008111.
Fan, Y., Li, H., and Miguez-Macho, G., 2013. Global patterns of groundwater table depth. *Science*, 339 (6122), 940–943. doi:10.1126/science.1229881.
Gleeson, T., et al., 2011. Mapping permeability over the surface of the Earth. *Geophysical Research Letters*, 38 (2), L02401. doi:10.1029/2010GL045565.
GRASS Development Team, 2020. Geographic resources analysis support system (GRASS) software, version 7.8.
Gustard, A., Bullock, A., and Dixon, J.M., 1992. *Low flow estimation in the United Kingdom*. Wallingford: Institute of Hydrology.
Habets, F., et al., 2008. The SAFRAN-ISBA-MODCOU hydrometeorological model applied over France. *Journal of Geophysical Research*, 113 (D6), D06113. doi:10.1029/2007JD008548.
Jacob, D., et al., 2014. EURO-CORDEX: new high-resolution climate change projections for European impact research. *Regional Environmental Change*, 14 (2), 563–578. doi:10.1007/s10113-013-0499-2.
Jacob, D., et al., 2020. Regional climate downscaling over Europe: perspectives from the EURO-CORDEX community. *Regional Environmental Change*, 20 (2), 51. doi:10.1007/s10113-020-01606-9.
Langevin, C.D., et al., 2017. *Documentation for the MODFLOW 6 groundwater flow model*. Documentation for the MODFLOW 6 Groundwater Flow Model. Reston, VA: U.S. Geological Survey, USGS Numbered Series No. 6-A55.
Lanini, S., et al., 2019. Recharge des aquifères à l'échelle de la France : estimation, évolution et incertitudes associées. In: *Colloque SHF-UNESCO : sécheresses, étiages et déficits en eau*, Paris, France. https://hal.archives-ouvertes.fr/hal-02159826
Lanini, S. and Caballero, Y., 2016. Groundwater recharge and associated uncertainty estimation combining multi-method and multi-scale approaches. *International Congress on Environmental Modelling and Software*.
Le Bas, C., 2020. Carte de la Réserve Utile en eau issue de la Base de Données Géographique des Sols de France.
Ledoux, E., et al., 1989. Spatially distributed modeling: conceptual approach, coupling surface water and groundwater. In: H.J. Morel-Seytoux, eds. *Unsaturated flow in hydrologic modeling: theory and practice*. Dordrecht: Springer Netherlands, 435–454.
Le Mesnil, M., et al., 2020. Interbasin groundwater flow: characterization, role of karst areas, impact on annual water balance and flood processes. *Journal of Hydrology*, 585, 124583. doi:10.1016/j.jhydrol.2020.124583
Le Moigne, P., et al., 2020. The latest improvements with SURFEX v8.0 of the Safran–Isba–Modcou hydrometeorological model for France. *Geoscientific Model Development*, 13 (9), 3925–3946. doi:10.5194/gmd-13-3925-2020.
Mardhel, V., Pinson, S., and Allier, D., 2021. Description of an indirect method (IDPR) to determine spatial distribution of infiltration and runoff and its hydrogeological applications to the French territory. *Journal of Hydrology*, 592, 125609. doi:10.1016/j.jhydrol.2020.125609
Maxwell, R.M., Condon, L.E., and Kollet, S.J., 2015. A high-resolution simulation of groundwater and surface water over most of the continental US with the integrated hydrologic model ParFlow v3. *Geoscientific Model Development*, 8 (3), 923–937. doi:10.5194/gmd-8-923-2015.
McKee, T.B., Doesken, N.J., and Kleist, J., 1993. The relationship of drought frequency and duration to time scales. In: *Proceedings of the 8th Conference on Applied Climatology*. MA: American Meteorological Society Boston, 179–183.
Miguez-Macho, G., et al., 2007. Incorporating water table dynamics in climate modeling: 2. Formulation, validation, and soil moisture simulation. *Journal of Geophysical Research*, 112 (D13), D13108. doi:10.1029/2006JD008112.
Muelchi, R., et al., 2021. River runoff in Switzerland in a changing climate – runoff regime changes and their time of emergence. *Hydrology and Earth System Sciences*, 25 (6), 3071–3086. doi:10.5194/hess-25-3071-2021.
Nash, J.E. and Sutcliffe, J.V., 1970. River flow forecasting through conceptual models part I — a discussion of principles. *Journal of Hydrology*, 10 (3), 282–290. doi:10.1016/0022-1694(70)90255-6.
Nistor, -M.-M., et al., 2018. LAND COVER AND TEMPERATURE IMPLICATIONS FOR THE SEASONAL EVAPOTRANSPIRATION IN EUROPE. *Geographia Technica*, 13 (1). doi:10.21163/GT_2018.131.09.
Office International de l'Eau, 2019. *Bulletin de situation hydrologique de janvier 2019*. France: Office International de l'Eau.
Pella, H., Sauquet, E., and Chandesris, A., 2006. Construction d'un réseau hydrographique simplifié à partir de la BD Carthage®. *Ingénierie*, 46, 3–14.
Rousset, F., et al., 2004. Hydrometeorological modeling of the Seine basin using the SAFRAN-ISBA-MODCOU system. *Journal of Geophysical Research*, 109 (D14), D14105. doi:10.1029/2003JD004403.
Seguin, -J.-J., 2015. *Proposition d'un indicateur piézométrique standardisé pour le Bulletin de Situation Hydrologique 'Nappes'. Rapport final*. Orléans, BRGM/RP-64147-FR, No. BRGM/RP-64147-FR.

Soubeyroux, J.-M., et al., 2021. *Les nouvelles projections climatiques de référence DRIAS 2020 pour la métropole*. Météo France. http://www.drias-climat.fr/document/rapport-DRIAS-2020-red3-2.pdf

Stollsteiner, P., 2012. *PROJET Explore 2070 - Evaluation de l'impact du changement climatique - Rapport final*. Orléans, BRGM/RP-61483-FR, No. BRGM/RP-61483-FR.

Taylor, K.E., Stouffer, R.J., and Meehl, G.A., 2012. An overview of CMIP5 and the experiment design. *Bulletin of the American Meteorological Society*, 93 (4), 485–498. doi:10.1175/BAMS-D-11-00094.1.

Terray, L. and Boé, J., 2013. Quantifying 21st-century France climate change and related uncertainties. *Comptes Rendus Geoscience*, 345 (3), 136–149. doi:10.1016/j.crte.2013.02.003.

Thiéry, D., 2015. *Code de calcul MARTHE - Modélisation 3D des écoulements dans les hydrosystèmes - Notice d'utilisation de la version 7.5 (MARTHE: modeling software for groundwater flows)*. Orléans, BRGM/RP-64554-FR, No. BRGM/RP-64554-FR.

Thiéry, D., Amraoui, N., and Noyer, M.-L., 2018. Modelling flow and heat transfer through unsaturated chalk – validation with experimental data from the ground surface to the aquifer. *Journal of Hydrology*, 556, 660–673. doi:10.1016/j.jhydrol.2017.11.041

Thiéry, D., Picot-Colbeaux, G., and Guillemoto, Q., 2020. *Guidelines for MARTHE v7.8 computer code for hydro-systems modelling (English version)*. Orléans, BRGM/RP-69660-FR, No. BRGM/RP-69660-FR.

Thornthwaite, C.W., 1948. An approach toward a rational classification of climate. *Geographical Review*, 38 (1), 55–94. doi:10.2307/210739.

van Vuuren, D.P., et al., 2011. The representative concentration pathways: an overview. *Climatic Change*, 109 (1), 5. doi:10.1007/s10584-011-0148-z.

Verfaillie, D., et al., 2017. The method ADAMONT v1.0 for statistical adjustment of climate projections applicable to energy balance land surface models. *Geoscientific Model Development*, 10 (11), 4257–4283. doi:10.5194/gmd-10-4257-2017.

Vergnes, J.-P., et al., 2012. A simple groundwater scheme for hydrological and climate applications: description and offline evaluation over France. *Journal of Hydrometeorology*, 13 (4), 1149–1171. doi:10.1175/JHM-D-11-0149.1.

Vergnes, J.-P., et al., 2020. The AquiFR hydrometeorological modelling platform as a tool for improving groundwater resource monitoring over France: evaluation over a 60-year period. *Hydrology and Earth System Sciences*, 24 (2), 633–654. doi:10.5194/hess-24-633-2020.

Vergnes, J.-P. and Decharme, B., 2012. A simple groundwater scheme in the TRIP river routing model: global off-line evaluation against GRACE terrestrial water storage estimates and observed river discharges. *Hydrology and Earth System Sciences*, 16 (10), 3889–3908. doi:10.5194/hess-16-3889-2012.

Vergnes, J.-P., Decharme, B., and Habets, F., 2014. Introduction of groundwater capillary rises using subgrid spatial variability of topography into the ISBA land surface model. *Journal of Geophysical Research: Atmospheres*, 119 (19), 11,065–11,086. doi:10.1002/2014JD021573.

Vidal, J., et al., 2010. A 50-year high-resolution atmospheric reanalysis over France with the Safran system. *International Journal of Climatology*, 30 (11), 1627–1644. doi:10.1002/joc.2003.

Wada, Y., et al., 2010. Global depletion of groundwater resources. *Geophysical Research Letters*, 37 (20). doi:10.1029/2010GL044571.

Westerhoff, R., White, P., and Miguez-Macho, G., 2018. Application of an improved global-scale groundwater model for water table estimation across New Zealand. *Hydrology and Earth System Sciences*, 22 (12), 6449–6472. doi:10.5194/hess-22-6449-2018.

Wunsch, A., Liesch, T., and Broda, S., 2022. Deep learning shows declining groundwater levels in Germany until 2100 due to climate change. *Nature Communications*, 13 (1), 1221. doi:10.1038/s41467-022-28770-2.

Zeng, Y., et al., 2018. Global land surface modeling including lateral groundwater flow. *Journal of Advances in Modeling Earth Systems*, 10 (8), 1882–1900. doi:10.1029/2018MS001304.

Appendix A

Basic concepts and equations of MARTHE

Groundwater flow

Groundwater flow is computed using a three-dimensional finite-volume numerical scheme for solving a hydrodynamic equation based on Darcy's law and mass conservation, over irregular rectangular grids, and with the possibility of nested grids.

Drainage network

The drainage network is organized as a hierarchical network of tributaries connected to each other from upstream to downstream of a river basin. Each tributary contains a fixed number of stream reaches. The flow direction is given by the Strahler order computed for each reach. Each reach can potentially exchange water with the water table (gaining or losing streams). The flow equation in each reach is written as:

$$\frac{dS}{dt} = Q_{up} + Q_{riv} + Q_r + Q_{io} - Q_{down} \quad \text{(A1)}$$

where S (m^3) is the water storage in the reach, Q_{up} ($m^3.s^{-1}$) is the flow from upstream reaches, Q_{down} ($m^3.s^{-1}$) is the flow in the downstream reach, Q_{riv} ($m^3.s^{-1}$) the river–aquifer exchanges, Q_r ($m^3.s^{-1}$) the surface runoff, and Q_{io} ($m^3.s^{-1}$) an optional term representing either injection into or withdrawal from the river. Each reach is assumed to have a rectangular cross-section with a width W (m) and a reach length L (m). The scheme in Fig. A1 describes the geometry of the rectangular channel considered in each river grid cell. Q_{down} ($m^3.s^{-1}$) is computed using the Manning-Strickler equation as follows:

$$Q_{down} = \frac{1}{n} WLR^{2/3}\sqrt{s} \quad \text{(A2)}$$

where n is the dimensionless Manning friction factor and R (m) is the river hydraulic radius, computed as follows:

$$R = \frac{WL}{W+2H_{riv}} \quad \text{(A3)}$$

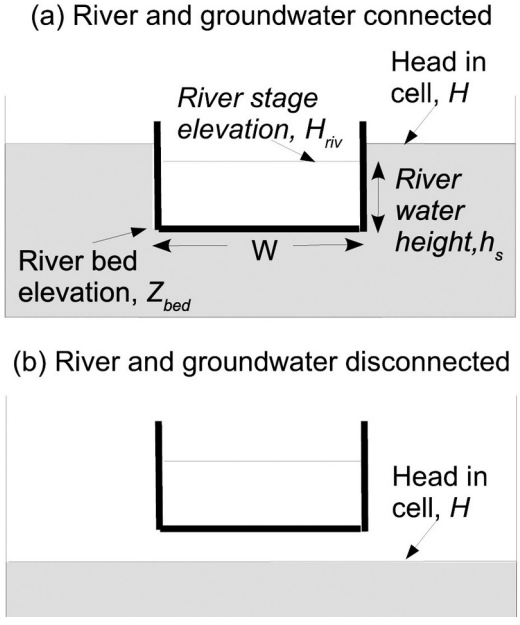

Figure A1. River–aquifer exchanges for (a) river and groundwater connected and (b) river and groundwater disconnected (Vergnes and Decharme 2012).

Table A1. Mean transmissivity and effective porosity values used in the model depending on lithology and taken from the scientific literature.

Lithology	Transmissivity ($m^2.s^{-1}$)	Effective porosity ($m^3.m^{-3}$)
Clay	5×10^{-4}	0.01
Limestone	5×10^{-3}	0.03
Chalk	1×10^{-2}	0.05
Sandstone	2×10^{-2}	0.07
Sand	5×10^{-2}	0.1

$$h_s = \frac{S}{WL} \quad \text{(A4)}$$

H_{riv} (m) is the river stage elevation corresponding to the sum of h_s (m), the variable river height in the rectangular channel, and the fixed riverbed elevation Z_{bed} (m); h_s is computed using Equation (A4) from S. Z_{bed} is defined as the elevation in the grid cell minus the critical river bankfull height h_c (m) as defined in Decharme *et al.* (2012). Combining these equations gives the implicit equation $h_s = \frac{S}{WL}$ which is solved iteratively in the whole river network using the Strahler order of each reach (Thiéry 2015, Thiéry *et al.* 2020).

River–aquifer exchanges

River–aquifer exchanges are represented through the concept of a river coefficient RC, commonly used in a majority or regional groundwater models for representing river–aquifer exchanges (Ledoux *et al.* 1989, Langevin *et al.* 2017). The fundamental assumption of this method is to consider that head losses between the stream and the aquifer are limited to those across the stream bed itself. The parameterization of river–aquifer exchanges is therefore:

$$Q_{riv} = \begin{cases} RC(H - H_{riv}) & \text{where } H > Z_{bed} \ (a) \\ RC(Z_{bed} - H_{riv}) & \text{where } H < Z_{bed} \ (b) \end{cases} \quad \text{(A5)}$$

where H (m) is the water table level. Equation (A5a) corresponds to the case where the water table is connected to the river. If the water table falls below the riverbed elevation, Equation (A5b) is applied and the river feeds the groundwater reservoir.

For a rectangular river channel characterized by a riverbed thickness b (m) and a hydraulic conductivity K_{riv} ($m.s^{-1}$), RC is equal to $LW(K_{riv}/b)$. As b and K_{riv} are generally poorly known, uncertainties in estimating the riverbed properties require adjusting this coefficient through model calibration. According to Vergnes *et al.* (2012), the b/K_{riv} (s) quantity represents the duration of water flow through the riverbed. This quantity can be approximated to a coefficient, τ (s), representing the time transfer coefficient between river and groundwater. Based on this assumption, RC becomes:

$$RC = \frac{LW}{\tau} \quad \text{(A6)}$$

River–aquifer exchanges are considered in both directions.

Appendix B

Details on the computation of the EPIR coefficient

For a non-influenced catchment without abstractions, anthropogenic water inputs, or inter-basin groundwater flow (Eakin 1966, Le Mesnil *et al.* 2020), the effective rainfall can be considered as the mean yearly stream flow. Assuming that the annual river baseflow is equal to the annual natural recharge of the aquifers from rainfall, the ratio of potential recharge to effective rainfall (effective rainfall infiltration ratio, EPIR) is equal to the ratio of baseflow to the mean yearly river flow, also called BFI for baseflow index (Gustard *et al.* 1992).

Estimating the EPIR at any point in a territory thus requires calculation of the BFI for each basin it contains, which is not feasible if the above conditions are to be met. For this reason, a statistical relationship was set between mean basin network development and persistence index values

(IDPR) (Mardhel *et al.* 2021). IDPR is a cartographic index, available for any point of France, and the mean BFI is calculated only for basins meeting the necessary conditions and with observed flow of good enough quality (Lanini and Caballero 2016, Caballero *et al.* 2022). Based on this relationship, it becomes possible to determine the EPIR values for each hydrogeological unit defined in the French BDLISA aquifer reference system (https://bdlisa.eaufrance.fr/, Brugeron *et al.* 2018). The EPIR is assumed to be constant for present and future periods.

Appendix C

Dataset and parameterization

River network

Grid cells with drainage basin areas < 330 km^2 were not considered river cells. This threshold value was based on a trial-and-error method in order to handle a reasonable number of tributaries while keeping a sufficiently detailed river network of 960 tributaries in the model. Figure 1 compares the modelled river network (grey network) with the reference river network (blue network) of the "BD Carthage" database (Pella *et al.* 2006) covering all of continental France. The Carthage rivers correspond to river lengths over 100 km, or rivers flowing into the sea with lengths over 25 km (class attributes equal to 1 in the BD Carthage database). The GMTED2010 DEM provides topographic data at a resolution of 7.5 arc seconds (grid cell width around 250 m). A bi-linear interpolation converts this DEM to a 2 km resolution grid for use in the model, defining the topography and subsequent river geometries.

Aquifer characteristics

Five main lithology units were selected in the domains where groundwater flow was simulated: clay, chalk, limestone, sandstone, and sand. Mean transmissivity and effective porosity values were chosen among the usual values, so as to be physically realistic, without being calibrated against field observations (Table A1).

The model contains only one superficial layer connected to streams and replenished by groundwater recharge. This single layer is divided into five domains (Fig. 1); their delineation relies on a method based on data cross-referencing between various hydrogeological and geological databases, including the World-wide Hydrogeological Mapping and Assessment Programme (WHYMAP; http://www.whymap.org), the International Geological Map of Europe (IGME) provided by the Federal Institute for Geosciences and Natural Resources at Hannover (BGR) (Asch 2005), and the simplified lithological map of France provided by BRGM, as well as a criterion based on the terrain slope. Regarding the slope value from the GMTED2010 elevation dataset, the model grid cells defined as mountainous were those having at least 70% of slopes ≥ 10% (0.1 m.m^{-1}) in the 30 arc second grid cell. Vergnes *et al.* (2012) used this methodology for retaining only the large sedimentary basins with regional hydrogeological systems, removing karst and basement rock areas (Brittany and Massif Central) and mountain areas.

River–aquifer exchanges

The time transfer coefficient between river and groundwater, τ (s), varies arbitrarily from 30 days in major rivers to 5 days in upstream grid cells. Its variation is controlled by a linear relationship with the stream order SO given by the river network in each grid cell of a given basin (Arora *et al.* 2001, Decharme *et al.* 2010, Vergnes *et al.* 2012):

$$\tau = \tau_{max} + (\tau_{min} - \tau_{max})\left[\frac{SO_{max} - \min(SO,\ SO_{max})}{SO_{max} - SO_{min}}\right] \quad \text{(C1)}$$

where $SO_{\max}$ and $SO_{\min}$ are the maximum and minimum stream order of the given basin, respectively. At a 2 km grid resolution over France, $SO_{\max}$ is equal to 50 and $SO_{\min}$ is equal to 1.

In a similar manner, the roughness coefficient n from the Manning equation (Equation A2) varies from 0.04 to 0.06 (upstream to downstream) in the river network of a given basin.

River width W is used when computing river flow, as well as for river–aquifer exchange parameterization. It is calculated through the empirical equation described by Decharme *et al.* (2012):

$$W = \max\left(10,\ 15Q_{yr}^{0.5}\right) \quad \text{(C2)}$$

where Q_{yr} is estimated for each grid cell using the mean simulated annual discharge values computed from effective rainfall. In a similar way, the river bankfull height h_c is computed using the following empirical equation (Decharme *et al.* 2012, Vergnes *et al.* 2014).

$$h_c = 1.4W^{0.28} \quad \text{(C3)}$$